Gaseous Phase Heat Capacity of Benzoic Acid

Luís M. N. B. F. Santos* and Marisa A. A. Rocha

Centro de Investigação em Química, Departamento de Química e Bioquímica, Faculdade de Ciências, Universidade do Porto, Rua do Campo Alegre, 687, P-4169-007 Porto, Portugal

Lígia R. Gomes

CIAGEB, Faculdade de Ciências de Saúde Escola Superior de Saúde da UFP, Universidade Fernando Pessoa, Rua Carlos da Maia, 296, P-4200-150 Porto, Portugal, and REQUIMTE, Departamento de Química e Bioquímica, Faculdade de Ciências, Universidade do Porto, Rua do Campo Alegre, 687, P-4169-007 Porto, Portugal

Bernd Schröder and João A. P. Coutinho

CICECO, Departamento de Química, Universidade de Aveiro, Campus Santiago, P-3810-193 Aveiro, Portugal

The gaseous phase heat capacity of benzoic acid (BA) was proven using the experimental technique called the "in vacuum sublimation/vaporization Calvet microcalorimetry drop method". To overcome known experimental shortfalls, the gaseous phase heat capacity of BA monomer was estimated by ab initio calculations and compared with experimental results. Gaseous phase heat capacities of BA were directly derived via calculated harmonic frequencies obtained by density functional theory (DFT) (B3LYP, BLYP, BP86, with 6-311++G(d,p), TZVP, cc-pVTZ basis sets) and the second-order Møller−Plesset theory, MP2/6-311++G(d,p). To increase the accuracy of estimation of the thermal properties, a procedure based on the calculation of the heat capacity from quantum chemical calculations in combination with a heat capacity balance of isodesmic reactions is described and applied to calculate the gaseous phase heat capacity, $C_{p,\mathrm{m}}$, of the monomeric species over the temperature range of (298.15 to 600) K. The gaseous phase thermodynamic properties of the monomeric form of the BA were also derived from the assignment of the fundamental vibrational frequencies using experimental IR spectra. An excellent agreement among the experimental gaseous phase heat capacities, the results obtained using the proposed ab initio procedure, and the results derived from the assignment of fundamental vibrational frequencies was found. The results for the monomeric form of the BA, directly or indirectly obtained, and conclusions of this work strongly support the thesis that the gaseous phase heat capacity data as currently found in the literature are underestimated to the order of 20 %.

Introduction

In calorimetry, benzoic acid (BA) is widely used as a test substance, a calibrant, and a primary standard reference. It is a recommended test substance for the evaluation of the performance of calorimeters, used for the measurements of heat capacities of solids, ranging from low temperatures to temperatures slightly above ambient.[1,2] BA has been further recommended as a primary reference standard for sublimation enthalpy measurements of substances having a vapor pressure of approximately 0.1 Pa at 298.15 K[3−6] or (10 to 360) Pa in the temperature range of (338 to 383) K. The application of BA as a sublimation enthalpy reference material caused controversy: some works[7,8] pointed out that the acid is not totally monomeric in gaseous phase. Nevertheless, BA is still to be considered as a suitable reference material, when measured under the conditions specified above. Therefore, it continues to be used as such. BA is also known as a recommended calibrant for enthalpies of fusion, for both adiabatic calorimetry and differential scanning calorimetry. Currently, BA is recommended as a secondary

reference material, primarily because of the poor agreement observed between the calorimetric values and those obtained by other methods.[9] Despite the reported uncertainty of about ± 3 % on vapor pressure data, BA was also recommended as a reference material for vapor pressure measurements.[10] The uncertainties in thermodynamic values of BA are associated to the uncertain experimental determination of its gas-phase thermodynamic properties. Because of its low volatility, direct determination in the gas phase is difficult; experimental vibrational spectroscopy becomes a method of choice.

Solid state X-ray studies[11] proved that BA occurs in dimeric form and that the −COOH moiety is planar with respect to the aromatic ring. Vibrational spectroscopy studies of BA have been conducted, in the condensed phase, via IR,[12] far-IR,[13] and Raman spectroscopy[14] and with BA trapped in low-temperature inert matrices.[15,16] IR studies in solution also indicate the existence of a dimer.[17] The structure of isolated BA in the gas phase has not been established unambiguously. Taking the interpretation of gaseous BA spectra obtained from microwave measurements, Onda et al.[18] suggested the presence of a species with a planar structure (equilibrium conformation) whose acid hydrogen is located close to the benzene ring, opposite to the

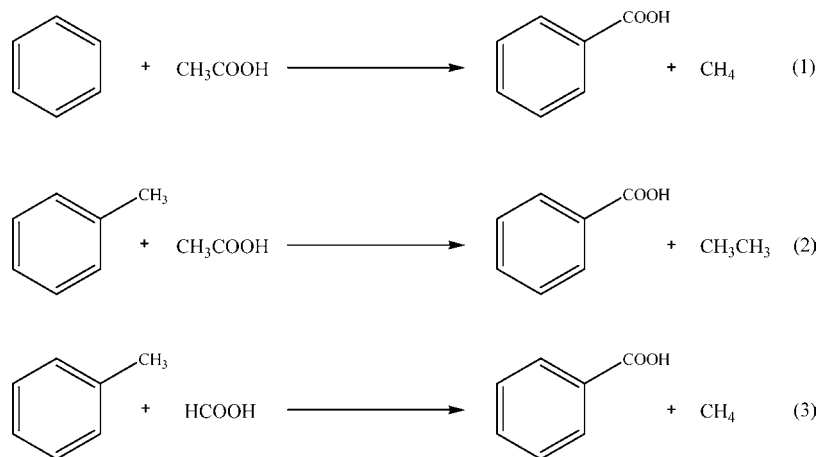* Corresponding author. Tel.: +351 220402536. Fax: +351220402659. E-mail: lbsantos@fc.up.pt.

Figure 1. Reaction schemes used in the isodesmic ab initio estimation procedure of the gaseous phase molar heat capacity of BA. (1) reaction scheme 1; (2) reaction scheme 2; (3) reaction scheme 3.

structure observed in the solid state where the hydrogen atom participates on the $R^2_2(8)$ ring of the dimeric species. To elucidate the molecular structure of gaseous BA, recent studies combining electron diffraction and theoretical calculations in the gas phase suggested that the carboxyl group is planar with respect to the phenyl ring and that the O—H group is eclipsed with respect to the C=O bond.[19] IR absorption spectroscopy of the jet-cooled BA showed that the substance exists in both its monomeric and dimeric form.[17]

Standard statistical mechanical methods were also widely used to calculate gaseous thermodynamic properties. The system's thermodynamic properties are modulated by means of a rigid-rotor harmonic oscillator (HO) model, modified, when necessary, to take into account the internal rotations of the molecule. Several theoretical ab initio studies were performed, to access the structural features of BA as a monomer, and the computation of their frequencies was presented by several authors.[20−27] In theoretical work, difficulties in the assignment of geometry and especially fundamental frequencies of the substance in gas phase are arising, also because of the lack of rigorous experimental data in the gaseous phase. The terms for the assignment of internal rotational energy levels for the molecular partition function, that allow the calculation of absolute heat capacities at constant volume, can be taken from spectroscopic data when available; otherwise, other approaches have to be considered. Statistical thermodynamic calculations performed later on seemed to be error-prone.[28] Because of error propagation, it is not recommended to use these data while estimating the thermodynamic properties of aromatic carboxylic acids for which experimental values are unknown. Therefore, both experimental and theoretical determinations of the heat capacity and entropy of gaseous BA are associated with high uncertainties. In fact, a discrepancy for the gas-phase heat capacity data of BA in the tables of Stull et al.[29] is known. The authors pointed out that these values were calculated from the preliminary assignments of vibrational frequencies. Later on, these data were reproduced in other data compilations, like the tables of Frenkel et al.[30] The values for the above-mentioned quantities are significantly different from those calculated by the simple additive method (including the correction for the hindered or free rotors), presented in reaction schemes 1, 2, and 3 (Figure 1).

In this work, the theoretical gaseous phase heat capacity, $C_{p,m}$, of BA is calculated, exploring a method that combines ab initio calculations with isodesmic reactions, joining theoretical with experimental data, to overcome the experimental and theoretical

drawbacks, causing erroneous estimates of the thermodynamic properties of the BA monomer in the gaseous phase. The application of isodesmic reactions methodology for the calculation of ideal-gas heat capacity is, as far as we know, proposed for the first time in the literature.

The proposed methodology is applied to the calculation of the gaseous phase heat capacity, $C_{p,m}$, of the monomeric species over a given temperature range of (298.15 to 600) K. The temperature dependence of the heat capacity of the BA monomer is derived from the results of geometry optimization of the molecule at a sufficient descriptive level of theory, followed by harmonic vibrational frequency calculations. Isodesmic and homodesmic reactions are applied once the relative values are tested and calculated with good reliability. In the isodesmic reaction approach,[31−33] all of the used species involved in the reactions are independently optimized followed by independent harmonic vibrational frequency calculations by a variety of computational methods. It is expected that inherent, method specific flaws cancel out in the overall balance of the chosen isodesmic reaction. Furthermore, applying an overall averaging procedure, a most precise temperature-dependent heat capacity function of the BA monomer is derived. Following the proposed methodology which incorporates the hypothetical isodesmic reaction approach, three such reactions have been designed, according to the schematic reactions presented in Figure 1.

Quantum Chemical Calculations

Geometry optimizations and the fundamental vibrational frequency calculations were performed at the following levels of theory: (i) Becke's functional in combination with the Lee et al. correlation function as the hybrid exchange-correlation energy functional (BLYP);[34,35] (ii) Becke's three-parameter exchange functional in combination with the Lee et al. correlation function as the hybrid exchange-correlation energy functional (B3LYP);[34,36] (iii) Becke−Perdew functional BP86[34,37] model chemistries containing 6-311++G(d,p),[38,39] TZVP,[40,41] and cc-pVTZ[42] basis sets. The second-order Møller−Plesset theory (MP2)[43] using the 6-311++G(d,p) basis set was additionally used. For each optimized structure, no imaginary modes were encountered, suggesting that an energetic minimum was obtained in all cases.

Gaseous phase heat capacities of BA were derived directly via calculated harmonic frequencies, starting from $T = 298.15$ K, at 100 K intervals in the (298.15 to 600) K range, applying scaling factors for the correction of anharmonicity, as indicated

Table 1. Applied Anharmonicity Scaling Factors for the Correction of the Vibrational Frequencies for the Different Quantum Chemical Models

model/basis set	anharmonicity scaling factors	ref
B3LYP/6-311++G(d,p)	0.9688	55
B3LYP/TZVP		
BLYP/6-311++G(d,p)	1.0001	55
BLYP/TZVP		
BP86/6-311++G(d,p)	0.9978	55
BP86/TZVP		
B3LYP/cc-pvtz	0.9661	90
BLYP/cc-pvtz	0.9970	90
BP86/cc-pvtz	0.9978	55
MP2/6-311++G(d,p)	0.9523	55

in Table 1. For all of the methods with standard basis sets, currently recommended scaling factors have been used. Some calculations of the ideal-gas thermodynamic functions were done using the Perl Script THERMO PL.[44] All quantum calculations were performed using the Gaussian 03 software package.[45]

Calvet Microcalorimetry

The total enthalpy change of BA, associated with the process, $\Delta_{cr,298.15K}^{g,T}H_m^o$, was determined using a high-temperature Calvet microcalorimeter, Setaram HT1000D, applying a similar technique of the drop method described by Skinner et al.[46] The measurement procedure and the description of the apparatus was described in detail by Santos et al.[4]

The value of $\Delta_{cr,298.15K}^{g,T}H_m^o$ can be subdivided in the enthalpy change because of the heating of the sample, in its respective condensed phase, the fusion of the sample, if the hot-zone temperature exceeds the fusion temperature of the compound, $\Delta_{298.15\,K}^{T}H_m^o(cd)$, and the vaporization process of the sample at the hot-zone temperature, $\Delta_f^g H_m^o(T)$, as illustrated in Figure 2:

Samples of about (5 to 6) mg of BA were placed into thin capillary tubes, sealed at one end, and dropped simultaneously with a corresponding blank tube at room temperature into the hot reaction zone of the calorimeter. The heating of the sample from room temperature to the hot-zone temperature is observed as an endothermic peak. When the calorimetric cells reach thermostability, the sample is removed from the hot zone by vaporization into a vacuum. The capillary tubes were weighted on a Mettler Toledo XS-105 dual range analytical balance with a sensitivity of $1 \cdot 10^{-5}$ g. The blank heat capacity corrections were performed because of differences in the mass of both capillary tubes and the different sensibilities of the two calorimetric cells.

The gaseous phase enthalpy change from $T = 298.15$ K to the hot-zone temperature T, $\Delta_{298.15K}^{T}H_m^o(g)$, was calculated using the following equation:

$$\Delta_{298.15K}^{T}H_m^o(g) = \Delta_{cr,298.15K}^{g,T}H_m^o - \Delta_{cr}^{g}H_m^o(BA, T = 298.15\ K) \quad (1)$$

where $\Delta_{cr,298.15K}^{g,T}H_m^o$ corresponds to the total enthalpy change for the process and $\Delta_{cr}^{g}H_m^o(BA, T = 298.15$ K) represents the standard molar enthalpy of sublimation of BA. The recommended value is $\Delta_{cr}^{g}H_m^o(BA, T = 298.15$ K) = (89.70 ± 1.00) kJ·mol^{-1}.[6]

Results and Discussion

In their systematic study on diatomic molecules, Sinnokrot and Sherrill[47] have shown that B3LYP is able to accurately predict vibrational frequencies. Nevertheless, the problems caused by general anharmonic vibrations in polyatomic molecules were not part of their work. The perturbation theory

treatment makes the determination of quadratic force constants possible, by means of numerical differentiation of analytical second derivatives with respect to normal coordinates that can be applied for the calculation of anharmonic vibrational constants. Neugebauer and Hess[48] suggested that different exchange correlation functionals, namely, B3LYP and BP86 combined with TZVP, may be applied in density functional theory (DFT) calculations of vibrational spectra of polyatomic asymmetric molecules. Also, at the B3LYP level of theory, both 6-31+G(d) and 6-311+G(d,p) basis sets were used to select different geometries as the most stable conformer for alkanes, ethers, and alcohols.[47] Dunning and Woon[49,50] also included diffuse functions (cc-pVTZ and aug-cc-pVTZ) on the correlation for computation of conformational energies of dipropylether.

In this work, the computation of geometric minima and the corresponding harmonic vibrational frequencies for BA was done at several levels of theory that combined B3LYP, BLYP, BP86, and MP2 with the 6-311++G(d,p)/cc-pVTZ/TZVP basis sets. The geometric parameters obtained for the monomer species are in agreement with those previously reported.[22,51] Geometry optimizations and frequency calculations of acetic acid (CH_3COOH), benzene (C_6H_6), ethane (CH_3CH_3), formic acid (HCOOH), methane (CH_4), and toluene ($C_6H_5CH_3$) were made, to derive the gaseous phase heat capacity of BA based on isodesmic reactions as represented in reactions schemes 1 to 3 (Figure 1).

Scaling Factors for Harmonic Vibrational Frequencies

The scaling factors applied for the intake of harmonic fundamental vibrational frequencies varied with the computational model used and are shown in Table 1. Harmonic frequency scaling factors for vibrations have been subject of study and evaluation during recent years. Andersson and Uvdal[52] reported on the B3LYP scaling factor convergence: the scaling factors, applied to B3LYP, did not change significantly when evaluated for basis sets larger than 6-311+G(d,p), so they recommend the scaling factor of the latter for B3LYP calculations involving larger basis sets. The evaluation of harmonic frequency scaling factors for B3LYP, BLYP, and MP2 for the polarized valence triple-ζ, Sadlej pVTZ base was done.[53] Harmonic vibrational frequencies computed at the B3LYP/TZV2P level of theory were scaled by a factor of 0.9688 as recently recommended.[54]

Merrick et al.[55] recently reported a study concerning the evaluation of frequency scaling factors for the prediction of fundamental and low vibrational frequencies, as well as for zero-point vibrational energies and thermal contributions to computed enthalpies and entropies by statistical thermodynamics. They observed that hybrid DFT procedures perform well in the calculation of low-frequency vibrations as well as for the vibrational component of the thermal contribution to enthalpies and entropies, $\Delta H_{vib}(T)$ and $S_{vib}(T)$. In the same work, the authors discouraged the use of MP2 with small basis sets that include diffuse functions for the prediction of low frequencies. The effect of varying the percentage of exact exchange shows a behavior analogous to that found for normal fundamental frequencies. Hybrid DFT procedures also seem to perform well when compared to other higher computational cost models, like a coupled cluster with single and double excitation (CCSD) or a quadratic configuration interaction with single and double excitation (QCISD).

Internal Rotation Treatment

In spite of the recurrence of isodesmic reactions as a reliable method, the proposed methodology for the achievement of a
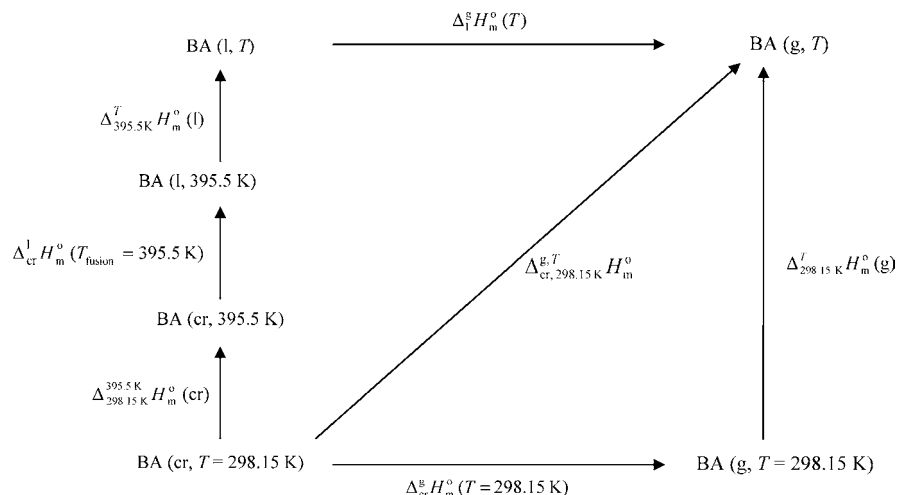
Figure 2. Hypothetical thermodynamic cycle for the heating, fusion, and vaporization/sublimation experiment of BA used for the experimental determination of the gaseous phase molar heat capacity of the BA.

suitable value for $C_{p,m}$ of BA depends on the computation of the heat capacity values ($C_{p,m}$) of several substances.

Concerning molecular partition functions in ab initio based predictions of thermodynamic properties, all rotations were first treated as harmonic, for all species. The standard HO approach seems to be adequate for obtaining the coefficients for the partition function when aromatic and unsaturated organic molecules are under study, but for single bonded molecules that exhibit internal rotations with higher amplitudes, the computation of the hindered rotor (HR) contribution is advisable, to correct for the respective partition function. The partition function for the internal rotations depends on the way the kinetic and potential energies of the system are calculated. In the one-dimensional approach (1D-HR), the usual approximation for the potential energy is used: for each internal rotation, a one-dimensional potential energy curve (1D-PES) is calculated, and the total multidimensional potential energy surface (mD-PES) is assumed to be the sum of these one-dimensional contributions.[56] This seems to be the case for some of the molecules used in the isodesmic reactions, namely, acetic acid and ethane, that can exhibit rotational potential barriers of the RT magnitude. In the HR model, the assignment of internal rotational energy levels for each rotor uses both an internal rotational constant and a reduced moment of inertia of the constrained rotation group. There are several ways to insert the internal rotations into the HO model, and several approaches have been suggested to overcome that difficulty.[57−70] The 1D-HR model which allows the partition function to take over the internal rotational partition term for free rotation and for constrained rotations was further applied for acetic acid and ethane, and the free rotor model was used in the case of the methyl group in toluene. In accordance with experimental findings,[71−74] the methyl and OH rotations of acetic acid were treated as an HR, using the approach proposed by Ayala and Schlegel,[73] as implemented in the Gaussian 03 software package. It was found that the heat capacity contribution obtained using the HR treatment, for the OH rotation (associated to the frequency around 660 cm^{-1}) is, for the working temperature range, identical to the value obtained from an HO partition function. In ethane, the known potential barrier[75,76] hindering the free rotation of the methyl group around the C−C bond was taken into account, using the Ayala and Schlegel approach. The methyl group in toluene was considered to be a free rotor[77] and was treated accordingly.[78−82] As it was observed in acetic acid, the heat capacity contribution

Table 2. Calculated Molar Gaseous Phase Heat Capacities, $C_{p,m}$, Obtained for BA (C_6H_5COOH) at Constant Pressure, Derived from the Calculated Frequencies after Anharmonicity Correction Using the Scaling Factors Presented in Table 1

T/K	298.15	300	400	500	600
	C_p/J·K^{-1}·mol^{-1}				
B3LYP/6-311++G(d,p)	126.6	127.4	164.6	195.3	219.5
BLYP/6-311++G(d,p)	127.2	127.9	165.2	195.9	220.1
BP86/6-311++G(d,p)	127.4	128.2	165.4	195.9	220.1
MP2/6-311++G(d,p)	131.7	132.5	169.2	199.1	222.7
B3LYP/cc-pvtz	126.2	126.9	164.2	194.9	219.2
BLYP/cc-pvtz	126.6	127.3	164.6	195.3	219.6
BP86/cc-pvtz	126.5	127.2	164.5	195.1	219.4
B3LYP/TZVP	126.8	127.5	164.7	195.3	219.5
BLYP/TZVP	127.2	128.0	165.2	195.8	220.0
BP86/TZVP	127.6	128.4	165.5	196.0	220.1

obtained using the HR treatment for the OH rotation in BA is similar to the value obtained from an HO partition function. The lowest vibration frequency of the BA was assigned to the axial torsion of the carboxylic group but was nevertheless treated as a rigid HO, taking into account, for the working temperature range (less than 600 K), the relatively high energy barrier (26 kJ·mol^{-1}, MP2/6-31G) and the energy profile of the rotation of the carboxylic group that was studied by several levels of theory, where the energy minima corresponds to planar configurations because of the resonance stabilization of the π-system.[83]

Ab initio Based Gaseous Phase Heat Capacities

Theoretical frequencies and modes were assigned by comparison according to the ones already assigned from IR spectral data obtained for BA.[16,22] The ab initio fundamental vibrational frequency data for each different theoretical model are available as Supporting Information (Table S1). For the monomeric form of the BA, the molar gaseous phase heat capacity results, obtained with different theoretical models, are presented in Table 2. The molar gaseous phase heat capacity results derived for the other molecular species involved in the isodesmic reaction schemes are presented as Supporting Information (Tables S2 to S7). Heat capacities are given at 298.15 K and in the temperature range between (298.15 and 600) K for the same level of theory using the scaling factors listed in Table 1.

In the cases of methane,[84] benzene,[85] and the BA[28,29] monomer, the heat capacity literature values have been compiled as such, with no further treatment. Table 3 lists the literature

Table 3. Literature Molar Gaseous Phase Heat Capacities, $C_{p,m}$, at Constant Pressure (0.1 MPa) at Different Temperatures

T/K	298.15	300	400	500	600	ref
	$C_{p,m}$/J·K^{-1}·mol^{-1}					
acetic acid (CH$_3$COOH)	66.53	66.82	81.67	94.56	105.23	29, 30
formic acid (HCOOH)	45.68	45.84	54.52	62.63	69.81	71
benzene (C$_6$H$_6$)	82.44	83.02	113.52	139.35	160.09	85
toluene (C$_6$H$_5$CH$_3$)	103.70	104.40	139.90	170.80	196.20	79
methane	35.69	35.76	40.63	46.63	52.74	84
ethane	52.47	52.72	65.48	77.99	89.24	76

gaseous phase heat capacities at different temperatures for acetic acid, formic acid, benzene, toluene, methane, and ethane.

For all of the models or levels of theory, the direct calculated computational gaseous phase heat capacities for BA are significantly higher than the data listed in the Stull et al. tables.[29] This is valid for all levels of theory used, which gives rise to suspicions on the quality of the previously published data. Taking advantage of the error cancellation, an isodesmic reaction approach has been used for the calculation of gas-phase heat capacities. The direct heat capacities of BA in gaseous phase were obtained, on the basis of three hypothetical reaction schemes (Figure 1) as depicted in the following equations:

$$C_p(\text{BA}) = \Delta C_p(\text{reaction scheme 1, theoretical}) - \\ C_p(\text{CH}_4) + C_p(\text{CH}_3\text{COOH}) + C_p(\text{C}_6\text{H}_6) \quad (2)$$

$$C_p(\text{BA}) = \Delta C_p(\text{reaction scheme 2, theoretical}) - \\ C_p(\text{CH}_3\text{CH}_3) + C_p(\text{CH}_3\text{COOH}) + C_p(\text{C}_6\text{H}_5\text{CH}_3) \quad (3)$$

$$C_p(\text{BA}) = \Delta C_p(\text{reaction scheme 3, theoretical}) - \\ C_p(\text{CH}_4) + C_p(\text{HCOOH}) + C_p(\text{C}_6\text{H}_5\text{CH}_3) \quad (4)$$

In these equations, the theoretical $\Delta C_{p,m}$ values were calculated for each theoretical level of calculation according to the three reaction schemes. The $C_{p,m}$ values are literature data derived from statistical thermodynamics analysis and/or experimental data. Table 4 shows values obtained for absolute heat capacities for BA, $C_{p,m}$(BA), obtained with the proposed method for the three different isodesmic reactions and for all of the levels of theory considered in this work. Table 5 presents the average heat capacity data for each reaction scheme, the overall average for the theoretical gaseous heat capacity of BA, and the estimate based on the Joback group contribution method,[86] as well as the data found in the literature,[29,30] in the temperature interval from (298.15 to 600) K.

From the fitting of the derived ab initio data, the following gaseous phase molar heat capacity and enthalpy change from 298.15 K to T/K, for the monomeric form of BA, is proposed for the temperature interval from (298.15 K to 600) K:

$$C_{p,m}(T)/(\text{J·K}^{-1}\text{·mol}^{-1}) = -3.189167 \cdot 10^{-4}T^2 + \\ 5.947417 \cdot 10^{-1}T - 22.99 \quad (5)$$

$$[H_m(T) - H_m(298.15 \text{ K})]/(\text{kJ·mol}^{-1}) = \\ -1.063056 \cdot 10^{-7}T^3 + 2.973708 \cdot 10^{-4}T^2 - \\ 2.299417 \cdot 10^{-2}T - 16.76 \quad (6)$$

where T is the temperature in Kelvin.

Ideal Gas Thermodynamic Properties Derived from Experimental Vibrational Spectroscopy Data

Low temperature IR spectra in argon matrices of benzoic and deuterobenzoic acid monomers and dimers were recorded and interpreted by Stepanian et al.[16] and more recently by Bakker et al.[17] using jet-cooled IR spectra. For BA, a good agreement

Table 4. Calculated Gaseous Phase Heat Capacities, $C_{p,m}$, Obtained for BA (C$_6$H$_5$COOH) at Constant Pressure, Derived from the Hypothetical Isodesmic Reaction Procedures

		T/K	298.15	300	400	500	600
			$C_{p,m}$/J·K^{-1}·mol^{-1}				
B3LYP/6-311++G(d,p)	scheme 1		125.7	126.5	163.8	194.3	218.3
	scheme 2		126.0	126.8	164.0	194.2	218.1
	scheme 3		125.5	126.4	163.7	195.0	220.3
BLYP/6-311++G(d,p)	scheme 1		126.1	126.7	163.9	194.4	218.4
	scheme 2		126.3	127.0	163.9	194.2	218.1
	scheme 3		125.8	126.5	163.7	195.2	220.3
BP86/6-311++G(d,p)	scheme 1		125.9	126.7	163.8	194.3	218.4
	scheme 2		126.2	126.9	163.9	194.1	218.0
	scheme 3		125.6	126.5	163.8	195.0	220.4
MP2/6-311++G(d,p)	scheme 1		126.9	127.6	166.2	198.0	222.9
	scheme 2		127.2	127.9	164.5	194.5	218.4
	scheme 3		126.3	127.1	164.3	195.3	220.6
B3LYP/cc-pVTZ	scheme 1		125.7	126.3	163.6	194.1	218.1
	scheme 2		125.9	126.6	163.4	193.6	217.5
	scheme 3		125.5	126.1	163.5	194.9	220.2
BLYP/cc-pVTZ	scheme 1		125.9	126.5	163.8	194.3	218.2
	scheme 2		126.3	127.0	164.1	194.4	218.3
	scheme 3		125.6	126.2	163.6	194.9	220.1
BP86/cc-pVTZ	scheme 1		125.8	126.5	163.7	194.3	218.3
	scheme 2		125.9	126.5	163.4	193.7	217.7
	scheme 3		125.4	126.2	163.6	194.9	220.2
B3LYP/TZVP	scheme 1		126.0	126.7	163.8	194.4	218.3
	scheme 2		126.2	126.9	163.7	193.9	217.6
	scheme 3		125.7	126.5	163.8	195.2	220.4
BLYP/TZVP	scheme 1		126.1	126.9	163.9	194.3	218.5
	scheme 2		126.6	127.3	164.4	194.6	218.7
	scheme 3		125.7	126.6	163.8	195.0	220.5
BP86/TZVP	scheme 1		125.9	126.6	163.8	194.3	218.2
	scheme 2		126.3	127.0	164.0	194.3	218.2
	scheme 3		125.7	126.5	163.7	195.0	220.3

Table 5. Average Molar Heat Capacities, $C_{p,m}$, Results Obtained for BA (C$_6$H$_5$COOH), Derived from Reaction Schemes 1, 2, and 3, the Global Average, the Data Obtained by the Joback Method, and Literature Data

T/K	298.15	300	400	500	600
	$C_{p,m}$/J·K^{-1}·mol^{-1}				
literature[29,30]	103.47	104.01	138.36	170.54	196.73
Joback method[86a]	120.6	121.4	157.8	188.1	212.9
scheme 1[b]	126.0	126.7	164.0	194.7	218.8
scheme 2[b]	126.3	127.0	163.9	194.2	218.1
scheme 3[b]	125.7	126.5	163.8	195.0	220.3
average[b]	126.0	126.7	163.9	194.6	219.1

[a] Using the following group coefficients: (one) nonring [—COOH]; (five) ring [=C(H)—]; (one) ring [=C<], group coefficients. [b] This work.

was found between the two experimental vibrational spectra in most active fundamental vibrational resonances in the (500 to 1900) cm^{-1} region. In the present work, the fundamental vibrational frequencies, obtained by quantum chemical calculations, were assigned from the visual analysis of the displacement vectors as well as by comparison between the experimental and the theoretical relative absorption intensities. The present assignment compares well with the assignment proposed by Bakker et al.[17] and earlier by Stepanian et al.[16] and is presented in Table 6 for the B3LYP/6-311++G(d,p) and MP2/6-311++G(d,p) levels of theory, using the unscaled theoretical vibrational frequencies. Figure 3 shows the representation of the experimental vibrations, w_{exp}, as a function of the w_{calc}, obtained by B3LYP/6-311++G(d,p) and MP2/6-311++G(d,p) after frequency assignment in the range of (421 to 1752) cm^{-1}.

The complete fundamental vibrational frequency assignments are presented in Table 6, which are based on the experimental vibrational frequencies with the highest absorption intensities using the experimental data from Stepanian et al.[16] and the prediction of fundamental vibrational frequencies and assign-

Table 6. Experimental IR Spectral Data and Fundamental Vibrational Mode Assignment[a]

mode description (assignment)	16[b] w_{exp}/cm^{-1}	17[c] w_{exp}/cm^{-1}	B3LYP/6-311++G(d,p) w_{calc}/cm^{-1}	intensity	w_{pred}/cm^{-1}	MP2/6-311++G(d,p) w_{calc}/cm^{-1}	intensity	w_{pred}/cm^{-1}
C—O—O bend, out of plane			65	0.9	64	34	0.6	33
C—O—O bend, out of plane			159	0.8	156	146	1.0	143
C—O—O bend, in plane			216	1.5	212	216	1.4	212
C—O—O bend, in plane, ring deformation			383	4.8	376	383	4.4	375
C—C—C bend, out of plane			414	0.5	406	379	0.6	371
C—C—C bend, C—O—H bend, both out of plane	421		432	12.1	421	389	9.0	421
C—O—O bend, in plane			497	6.1	488	498	6.4	488
C—O—H bend, out of plane	568	571	576	71.5	568	526	79.4	568
C—C—C bend, in plane			632	0.2	620	621	0.1	609
C—O—H bend, in plane, ring deformation	628	631	640	48.9	628	638	35.0	628
C—C—H bend, out of plane ring	687	688	699	5.8	687	625	10.8	687
C—C—H bend (umbrella mode), out of plane ring	711	710	727	136.8	711	707	139.8	711
C—O—H bend, in plane, ring deformation	767	767	775	8.1	767	776	12.4	767
C—C—H bend, out of plane ring			824	0.1	809	767	1.5	753
C—C—H bend, out of plane ring			864	0.1	848	846	0.2	829
C—C—H bend, out of plane ring			960	1.7	942	900	1.2	882
C—C—H bend, out of plane ring			998	0.1	979	944	1.0	925
C—C—H bend, out of plane ring			1009	0.1	990	977	0.9	958
C—C—H bend, in plane ring			1018	0.4	999	1011	0.9	991
C—C—H bend, in plane ring	1027	1026	1046	20.6	1027	1046	17.1	1027
C—C—H bend, in plane ring	1066	1063	1089	114.7	1066	1094	85.8	1066
C—C—H bend, in plane ring	1086	1084	1114	44.5	1086	1119	63.4	1086
C—C—H bend, in plane ring			1185	0.6	1162	1184	0.1	1161
C—C—H bend, C—H—O bend, both in plane ring	1169	1173	1189	153.8	1169	1223	158.6	1169
C—C—H bend, C—H—O bend, both in plane ring	1185	1187	1211	86.7	1185	1199	41.7	1185
C—C—H bend, in plane ring			1340	2.1	1315	1460	1.6	1432
C—C stretch ring deformation								
C—C—H bend, in plane ring			1351	8.1	1325	1339	4.2	1313
C—C—H bend, C—H—O bend both in plane ring	1347	1347	1363	117.1	1347	1381	138.4	1347
C—C—H bend, in plane ring	1456	1455	1481	15.7	1456	1478	14.2	1456
C—C—H bend, in plane ring			1523	1.8	1494	1524	5.8	1495
C—C stretch, ring deformation	1590	1591	1622	5.3	1590	1630	5.6	1590
C—C stretch, ring deformation	1606	1609	1642	19.2	1606	1649	7.6	1606
C=O stretch, O—H bend in plane	1752	1752	1785	395.9	1752	1803	304.8	1752
C—H stretch	3012		3167	0.4	3012	3204	0.2	3012
C—H stretch	3041		3179	10.6	3041	3216	7.9	3041
C—H stretch	3068		3189	12.7	3068	3226	7.7	3068
C—H stretch	3079		3202	4.6	3079	3235	5.7	3079
C—H stretch	3098		3209	2.5	3098	3243	2.4	3098
O—H stretch	3567		3772	99.4	3567	3807	104.7	3567

[a] Full IR spectra derived from the prediction missing frequency modes from scaling the B3LYP/6-311++G(d,p) and MP2/6-311++G(d,p) frequency results of the experimental data. The prediction of vibrational frequencies, w_{pred}, was done by scaling the calculated frequencies [B3LYP/6-311++G(d,p) or MP2/6-311++G(d,p)] using the assigned experimental vibrational frequencies,[16] w_{exp}, in the range of (421 to 1752) cm^{-1}. $w_{pred} = 0.9812 w_{calc}$, using w_{calc} at B3LYP/6-311++G(d,p) level of theory. $w_{pred} = 0.9808 w_{calc}$, using w_{calc} at MP2/6-311++G(d,p) level of theory. [b] Stepanian et al.[16] [c] Bakker et al.[17]

ments, w_{pred}, for the lowest frequency and low absorption intensity modes that were derived from the scaled vibration frequencies [B3LYP/6-311++G(d,p) or MP2/6-311++G(d,p)]. The complete fundamental vibrational frequency modes and assignments using the same procedure based on the remaining theoretical models are available as Supporting Information (Table S1).

The ideal-gas standard ($p° = 10^5$ Pa) molar thermodynamic properties of the BA monomer were calculated by statistical thermodynamics,[87] using the assigned fundamental vibrational frequency data, derived from experimental spectra,[16] and the predicted vibrational frequencies obtained by B3LYP/6-311++G(d,p), as described above, are presented in Table 7. For the calculation of the vibrational contribution for the enthalpies and entropies, the lowest vibrational frequency of BA was assigned to the axial torsion of the carboxylic group but was treated as rigid HO as well as all of the other assigned vibrational frequency modes.

Table 8 lists the results obtained for the gaseous phase heat capacities of BA, $C_{p,m}$(BA), obtained by statistical thermodynamics, using the assigned vibrational fundamental frequency data, derived from experimental spectra[16] and the predicted vibrational frequencies at different theoretical models.

Calvet Microcalorimetry Gaseous Phase Heat Capacities

The results of the measurements of the total enthalpy change of BA associated with the process, $\Delta_{cr,298.15K}^{g,T}H_m^o$, as obtained from high-temperature Calvet microcalorimetry, and the calculated gaseous phase enthalpy change from $T = 298.15$ K to the hot-zone temperature T, $\Delta_{298.15K}^{T}H_m^o(g)$, are given in Table 9. Table 9 also presents the average gaseous phase heat capacity, C_p ($\langle T \rangle$), derived at the mean temperature of each temperature interval, and the estimated gaseous phase heat capacity for the overall average mean temperature weighted, based on the number of experiments at each temperature interval, is presented as well.

Conclusions

Figure 4 compares the values of the gaseous phase enthalpy change, from $T = 298.15$ K to the hot-zone temperature T, versus temperature, $\Delta_{298.15K}^{T}H_m^o(g) = f(T/K)$, obtained experimentally, the data derived from ab initio calculations in this work, the data derived by statistical thermodynamic using the assigned vibrational fundamental frequencies, and the data reported in the literature.[29,30] A good agreement among the
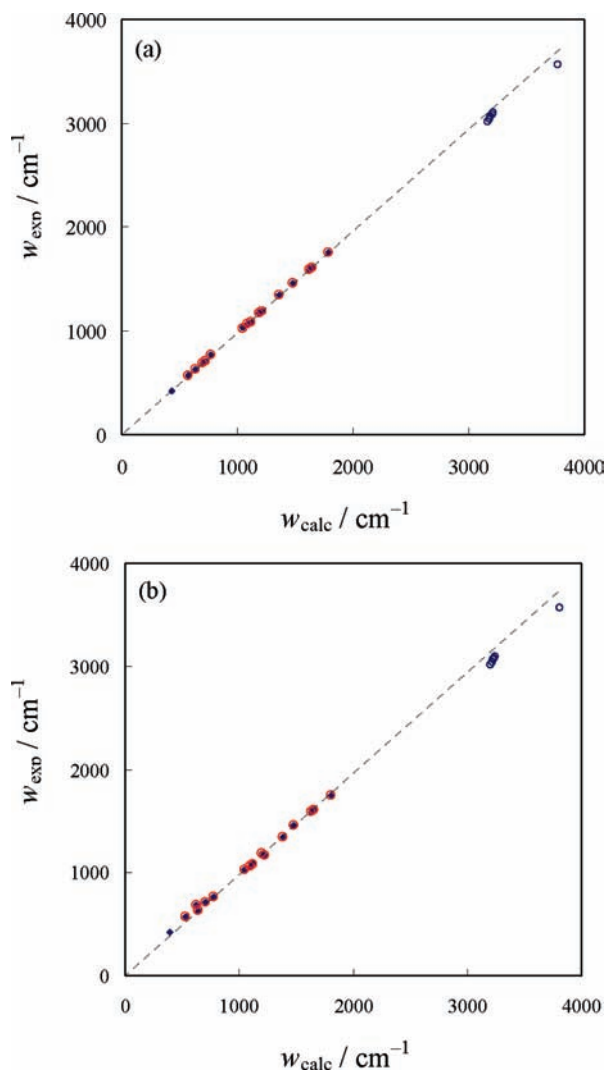
Figure 3. Plot of the calculated frequencies, w_{calc}, versus experimental vibrational frequencies,[16,17] w_{exp}, for the monomeric form of BA in the range (421 to 1752) cm^{-1}: (a) w_{calc} at the B3LYP/6-311++G(d,p) level of theory, $w_{pred} = 0.9812w_{calc}$; (b) w_{calc} at the MP2/6-311++G(d,p) level of theory, $w_{pred} = 0.9808w_{calc}$; blue ◆, plot between w_{exp} (Stepanian et al.) and w_{calc}; red ○, plot of w_{exp} (Bakker et al.) and w_{calc}; black ○, plot of w_{exp}, obtained by Stepanian et al., and w_{calc} for high vibrational frequencies (not considered in the above scaling fitting).

Table 7. Ideal-Gas Thermodynamic Properties for the BA (C$_6$H$_5$COOH) Monomer, Derived from the Experimental IR Fundamental Frequency Assignment Using the B3LYP/ 6-311++G(d,p) Level of Theory in the Prediction of the Low-Frequency and/or Low-Intensity Fundamental Frequency Modes ($p° = 10^5$ Pa)

T	$S°_m$	$C_{p,m}$	$[H°_m(T/K) - H°_m (0\ K)]$
K	J·K^{-1}·mol^{-1}	J·K^{-1}·mol^{-1}	kJ·mol^{-1}
100	267.2	54.1	4.2
200	313.9	86.5	11.2
298.15	355.6	125.1	21.5
300	356.4	125.8	21.8
375	387.5	154.1	32.3
400	397.8	162.9	36.2
450	417.9	179.1	44.8
500	437.5	193.6	54.1
525	447.1	200.2	59.1
600	475.1	218.1	74.8
700	510.2	237.6	97.6
800	543.0	253.5	122.2
900	573.6	266.6	148.2
1000	602.3	277.5	175.4

Table 8. Molar Gaseous Phase Heat Capacity Results of the Monomeric Form of BA (C$_6$H$_5$COOH), Derived from the Experimental IR Fundamental Frequency Assignment Using Different Computational Models for the Prediction of the Low-Frequency and/or Intensity Fundamental Frequency Modes^a

T/K	298.15	300	400	500	600
	$C_{p,m}$/J·K^{-1}·mol^{-1}				
EXP + B3LYP/6-311++G(d,p)	125.1	125.8	162.9	193.6	218.1
EXP + BLYP/6-311++G(d,p)	125.0	125.7	162.7	193.4	217.9
EXP + BP86/6-311++G(d,p)	125.4	126.1	163.1	193.7	218.2
EXP + MP2/6-311++G(d,p)	126.8	127.5	164.3	194.7	218.9
EXP + B3LYP/cc-pvtz	125.0	125.8	162.8	193.5	218.0
EXP + BLYP/cc-pvtz	124.8	125.5	162.4	193.2	217.7
EXP + BP86/cc-pvtz	125.2	125.9	162.8	193.5	218.0
EXP + B3LYP/TZVP	125.3	126.1	163.1	193.8	218.2
EXP + BLYP/TZVP	125.1	125.8	162.8	193.4	217.9
EXP + BP86/TZVP	125.6	126.3	163.3	193.9	218.3

^{a} Details and frequencies assignment available in Table S1 as Supporting Information.

results obtained by Calvet microcalorimetry, data derived from the isodesmic ab initio procedure, and the thermodynamic properties derived from the assigned fundamental vibrational frequencies was found. The data previously reported in the literature[29,30] are clearly in disagreement with the results obtained in this work, using different strategies.

Figure 5 compares the derived molar gaseous phase heat capacity, $C_{p,m}(\langle T\rangle)$, the estimate using the Joback group contribution method,[86] and the literature data. Figure S1, available as Supporting Information, presents a more extended comparison between the data derived in this work and some additional estimative methods. The results obtained by the Joback group contribution method are systematically 5 J·K^{-1}·mol^{-1} lower than the data derived in this work. The underestimation of Joback method is nevertheless acceptable taking into account the fact that the group coefficients for the carboxylic group used and available for the estimation of $C_{p,m}$ were attributed to a nonring group. Because of the uncertainty associated with the experimental data and the effective short experimental temperature interval for the derivation of $\Delta_{298.15K}^{T}H°_m(g)$ [from $T = (420$

to 466.8) K], it is difficult to evaluate or compare the experimental temperature dependency on the gaseous phase heat capacity of BA obtained experimentally. The temperature dependence of the heat capacity between the data derived in this work is in good agreement with the temperature dependence of the data estimated by the Joback group contribution method.

A good agreement among the experimental, ab initio, and spectroscopic results is observed. It is also interesting to notice the excellent agreement among the overall results for the experimental gaseous phase heat capacity, $C_{p,m}$(experimental, $T = 370.5$ K) $= 155 \pm 5$ J·K^{-1}·mol^{-1}, the ones derived by quantum chemical calculations at the same temperature (calculated using eq 5), $C_{p,m}$(theoretical, $T = 370.5$ K) $= 153.6$ J·K^{-1}·mol^{-1}, and the one derived from using the spectroscopic vibrational data frequency assignment (e.g., derived from B3LYP/6-311++G(d,p) level of theory), $C_{p,m}$(spectroscopic vibrational, $T = 370.5$ K) $= 153.7$ J·K^{-1}·mol^{-1}.

The derived gaseous phase heat capacity obtained in this work at 298.15 K, $C_{p,m}$(theoretical, $T = 298.15$ K) $= 126.0$ J·K^{-1}·mol^{-1}, compares quite well (1 % higher) with the one estimated using the vibrational frequency data assignment (obtained via IR spectroscopy in argon matrix[16]), $C_{p,m}$(spectroscopic vibrational, $T = 298.15$ K) $= 125.1$ J·K^{-1}·mol^{-1}. An uncertainty in the order of 1 % could be estimated, considering the comparative analysis between the gaseous phase molar heat capacity and the enthalpy change from 298.15 K to T/K,

Table 9. Experimental Results Obtained by Calvet Microcalorimetry for the Total Enthalpy Change, $\Delta_{\text{cr}, 298.15 \text{ K}}^{\text{g}, T} H_{\text{m}}^{\text{o}}$, the Calculated Gaseous Phase Molar Enthalpy Change from $T = 298.15$ K to the Hot-Zone Temperature T, $\Delta_{298.15\text{K}}^{T} H_{\text{m}}^{\text{o}}(\text{g})$, and the Derived Gaseous Phase Heat Capacity, $C_{p,\text{m}}(\langle T \rangle /\text{K})$ for the Monomeric Form of BA, at the Mean Temperature, $\langle T \rangle$

T	$\Delta_{\text{cr}, 298.15\text{K}}^{\text{g}, T} H_{\text{m}}^{\text{o}}$	$\Delta_{298.15\text{K}}^{T} H_{\text{m}}^{\text{o}}(\text{g})^a$	$\Delta_{298.15\text{K}}^{T} H_{\text{m}}^{\text{o}}(\text{g})^b$	$\langle T \rangle$	$C_{p,\text{m}}(\langle T \rangle /\text{K})^b$
K	kJ·mol^{-1}	kJ·mol^{-1}	kJ·mol^{-1}	K	J·K^{-1}·mol^{-1}
420.0	106.7	18.2	17.0	359.1	142 ± 5
	107.1		17.4		
	107.2		17.5		
	107.4		17.7		
	106.3		16.6		
456.0	114.9	24.5	25.2	377.1	162 ± 5
	116.0		26.3		
	115.2		25.5		
	114.7		25.0		
435.7	111.0	20.9	21.3	366.9	157 ± 5
	111.9		22.2		
	110.9		21.2		
446.8	111.5	22.9	21.8	372.5	151 ± 5
	112.6		22.9		
	112.5		22.8		
466.8	119.0	26.5	29.3	382.5	172 ± 5
	119.0		29.3		
	118.0		28.3		
				370.5^c	155 ± 5^c

^{a} Calculated by eq 6, obtained from the fitting of the derived ab initio data. ^{b} The gaseous phase molar enthalpy change from $T = 298.15$ K to the hot-zone temperature T uncertainty estimated as ± 1 % of the value. Gaseous phase molar heat capacity uncertainty estimated as ± 5 J·K^{-1}·mol^{-1}, based on the typical uncertainty of the $\Delta_{\text{cr}, 298.15 \text{ K}}^{\text{g}, T} H_{\text{m}}^{\text{o}}$ and excluding the uncertainty associated to the $\Delta_{\text{cr}}^{\text{g}} H_{\text{m}}^{\text{o}}(298.15$ K) of BA that corresponds to an systematic uncertainty in this methodology. ^{c} Overall gaseous phase heat capacity calculated for the weighted (based in the number of experiments) average temperature and heat capacity.
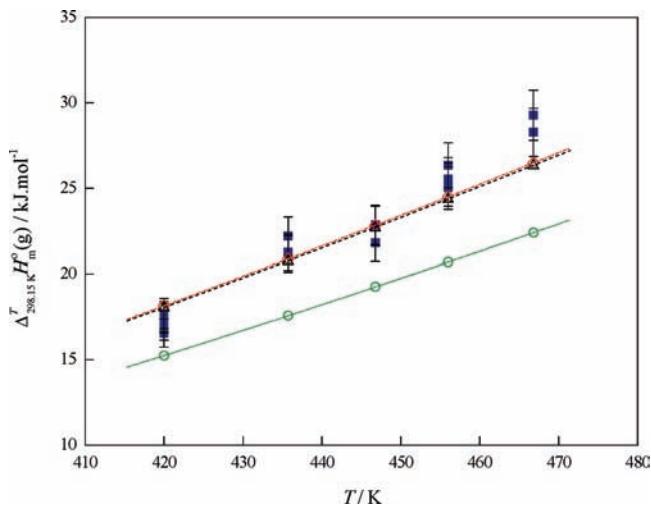

Figure 4. Plots of the gaseous phase enthalpy change data, from $T = 298.15$ K to the hot-zone temperature T, versus temperature, $\Delta_{298.15\text{K}}^{T} H_{\text{m}}^{\text{o}}(\text{g}) = f(T/K)$. Blue ■, experimental results obtained by Calvet microcalorimetry; red ◇, estimated from ab initio calculations (isodesmic procedure); blue △, derived from the experimental IR fundamental frequency assignment; green ○, reported in the literature.[29,30]

obtained experimentally and theoretically in this work, as presented in eqs 5 and 6.

The ideal gas standard ($p^{\circ} = 10^5$ Pa) molar absolute entropy of the BA monomer, at 298.15 K, $S^{\circ}_{\text{m}}(\text{g}, T = 298.15$ K) $= 355.6$ J·K^{-1}·mol^{-1}, derived by statistical thermodynamics, using the assigned fundamental vibrational frequency data, (Table 7) is in excellent agreement with the experimental result, $S^{\circ}_{\text{m}}(\text{g}, T = 298.15$ K) $= 355 \pm 2$ J·K^{-1}·mol^{-1}, calculated using the standard molar absolute entropy of solid BA at 298.15 K, $S^{\circ}_{\text{m}}(\text{cr},$
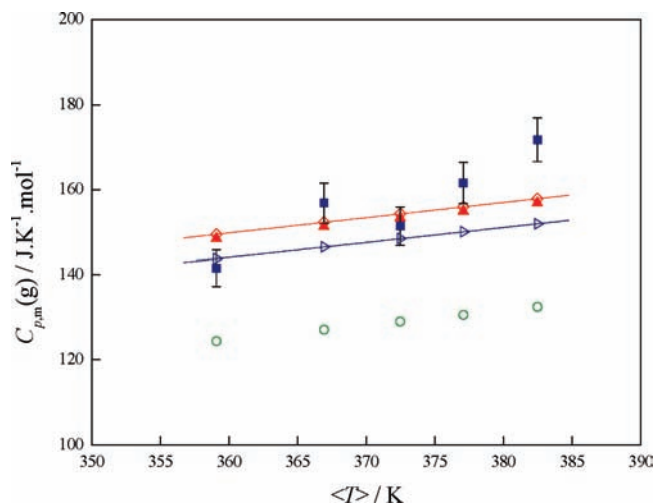

Figure 5. Plots of gaseous phase molar heat capacity results at the mean temperature, $\langle T \rangle = 0.5(T + 298.15)$, $C_{p,\text{m}}(\langle T \rangle /\text{K})$, between 298.15 K and the hot zone temperature of the Calvet microcalorimeter, versus mean temperature, $C_{p,\text{m}}(\langle T \rangle /\text{K}) = f(\langle T \rangle /\text{K})$: blue ■, experimental results obtained by Calvet microcalorimetry; red ◇, derived from ab initio calculations (isodesmic procedure); red ▲, derived from experimental IR fundamental frequency assignment; blue triangle pointing right, estimated by the Joback method;[86] green ○, reported in the literature.[29,30]

$T = 298.15$ K) $= 165.71$ J·K^{-1}·mol^{-1}, derived from adiabatic calorimetry,[88] and the standard molar entropy of sublimation at 298.15 K, determined by Knudsen effusion vapor pressure measurements, $\Delta_{\text{cr}}^{\text{g}} S^{\circ}_{\text{m}}(T = 298.15$ K) $= 189 \pm 2$ J·K^{-1}·mol^{-1}.[89]

In this work, new data for the ideal gas standard ($p^{\circ} = 10^5$ Pa) molar thermodynamic properties of the monomeric form of the BA are proposed. The results and conclusions reported here strongly support the thesis that the molar gaseous phase heat capacity of the monomeric form of BA, currently available in the literature, is underestimated to the order of 20 %. Some thermochemical and thermophysical literature data, which were derived or corrected using the previous literature data concerning the monomeric form of the BA (gaseous phase heat capacity or enthalpic correction), should be re-evaluated.

The application of the isodesmic reaction methodology for the calculation of ideal-gas heat capacity is proposed and applied for the calculation of the gaseous phase heat capacity of BA in the monomeric form. Using the same methodology, the ideal-gas thermodynamic properties of the BA dimer and the quantum chemical study of the dimerization equilibrium is in progress in our group.

Supporting Information Available:

The ab initio fundamental vibrational frequency data for each different theoretical model are available in Table S1. The molar gaseous phase heat capacity results derived for acetic acid, formic acid, benzene, toluene, ethane, and methane involved in the isodesmic reaction schemes are presented in Tables S2 to S7. Figure S1 presents a comparison between the data obtained by several estimative methods. This material is available free of charge via the Internet at http://pubs.acs.org.

Literature Cited

(1) McCullough, J. P.; Scott, D. W., Eds. *Experimental Thermodynamics, Vol. I: Calorimetry of Non-reacting System*; Butterworths: London, 1968; Chaps. 5, 6.
(2) Marsh, K. N., Ed. *Recommended Reference Materials for the Realization of Physicochemical Properties*; Blackwell: Oxford, 1987.
(3) Chickos, J. S.; Acree, W. E. Enthalpies of sublimation of organic and organometallic compounds. 1910−2001. *J. Phys. Chem. Ref. Data* **2002**, *31*, 537–698.

(4) Santos, L. M. N. B. F.; Schröder, B.; Fernandes, O. O. P.; Ribeiro da Silva, M. A. V. Measurement of enthalpies of sublimation by drop method in a Calvet type calorimeter: Design and test of a new system. *Thermochim. Acta* **2004**, *415*, 15–20.

(5) Cox, J. D. Recommended reference materials for realization of physicochemical properties. section: enthalpy. *Pure Appl. Chem.* **1974**, *40*, 424–426.

(6) Sabbah, R.; Xu-wu, A.; Chickos, J. S.; Planas Leitao, M. L.; Roux, M. V.; Torres, L. A. Reference materials for calorimetry and differential thermal analysis. *Thermochim. Acta* **1999**, *331*, 93–204.

(7) De Kruif, C. G.; Oonk, H. A. J. The determination of enthalpies of sublimation by means of thermal conductivity manometers. *Chem. Ing. Tech.* **1973**, *45*, 455–461.

(8) Murata, S.; Sakiyama, M.; Seki, S. Enthalpy of sublimation of benzoic acid and dimerization in the vapor-phase in the temperature range from 320 to 370 K. *J. Chem. Thermodyn.* **1982**, *14*, 723–731.

(9) Andon, R. J. L.; Connett, J. E. Calibrants for thermal analysis. Measurement of their enthalpies of fusion by adiabatic calorimetry. *Thermochim. Acta* **1980**, *42*, 241–247.

(10) van Genderen, A. C. G.; Oonk, H. A. J. The (solid + vapor) equilibrium. A view from the arc. *Colloid Surf., A* **2003**, *213*, 107–115.

(11) Bruno, G.; Randaccio, L. A refinement of the benzoic acid structure at room temperature. *Acta Crystallogr., Sect. B* **1980**, *36*, 1711–1712.

(12) Varsanyi, G. *Assignment for vibrational spectra of seven hundred benzene derivatives*; Adam Hilger: London, 1974; p 69.

(13) Kim, Y.; Machide, K. Vibrational spectra, normal vibrations and infrared intensities of six isotopic benzoic acids. *Spectrochim. Acta, Part A* **1986**, *42*, 881–889.

(14) Zelsmann, H. R.; Mielke, Z. Far-infrared spectra of benzoic acid. *Chem. Phys. Lett.* **1991**, *186*, 501–508.

(15) Reva, I. D.; Stepanian, S. G. An infrared study on matrix-isolated benzoic acid. *J. Mol. Struct.* **1995**, *349*, 337–340.

(16) Stepanian, S. G.; Reva, I. D.; Radchenko, E. D.; Sheina, G. C. Infrared spectra of benzoic acid monomers and dimers in argon matrix. *Vib. Spectrosc.* **1996**, *11*, 123–133.

(17) Bakker, J. M.; Aleese, L. M.; von Helden, G.; Meijer, G. The infrared absorption spectrum of the gas phase neutral benzoic acid monomer and dimer. *J. Chem. Phys.* **2003**, *119*, 11180–11185.

(18) Onda, M.; Asai, M.; Takise, K.; Kuwae, K.; Hayami, K.; Kuroe, A.; Mori, M.; Miyazaki, H.; Suzuki, N.; Yamaguchi, I. Microwave spectrum of benzoic acid. *J. Mol. Struct.* **1999**, *482*, 301–303.

(19) Aarset, K.; Page, E. M.; Rice, D. A. Molecular structures of benzoic acid and 2-hydroxybenzoic acid, obtained by gas-phase electron diffraction and theoretical calculations. *J. Phys. Chem. A* **2006**, *110*, 9014–9019.

(20) Boczar, M.; Szczeponek, K.; Wójcik, M. J.; Paluszkiewicz, C. Theoretical modeling of infrared spectra of benzoic acid and its deuterated derivative. *J. Mol. Struct.* **2004**, *700*, 39–48.

(21) Fillaux, F.; Romain, F.; Limage, M. H.; Leygue, N. Extended tunnelling states in the benzoic acid crystal: Infrared and Raman spectra of the OH and OD stretching modes. *Phys. Chem. Chem. Phys.* **2006**, *8*, 4327–4336.

(22) Palafox, M. A.; Núñez, J. L.; Gil, M. Theoretical Quantum Chemical Study of Benzoic Acid: Geometrical Parameters and Vibrational Wavenumbers. *Int. J. Quantum Chem.* **2002**, *89*, 1–24.

(23) Zielke, P.; Suhm, M. A. Raman jet spectroscopy of formic acid dimers: low frequency vibrational dynamics and beyond. *Phys. Chem. Chem. Phys.* **2007**, *9*, 4528–4534.

(24) Plazanet, M.; Fukushima, N.; Johnson, M. R.; Horsewill, A. J.; Trommsdorff, H. P. The vibrational spectrum of crystalline benzoic acid: Inelastic neutron scattering and density functional theory calculations. *J. Chem. Phys.* **2001**, *115*, 3241–3248.

(25) Shipman, S. T.; Douglass, P. C.; Yoo, H. S.; Hinkle, C. E.; Mierzejewski, E. L.; Pate, B. H. Vibrational dynamics of carboxylic acid dimers in gas and dilute solution. *Phys. Chem. Chem. Phys.* **2007**, *9*, 4572–4586.

(26) Wilmhurst, J. K. Infrared investigation of acetic acid and acetic acid-*d* vapors and a vibrational assignment for the monomeric acids. *J. Chem. Phys.* **1956**, *25*, 1171–1173.

(27) Furić, K.; Colombo, L. Vapour-phase Raman spectra of benzoic acid. *J. Raman Spectrosc.* **2005**, *17*, 23–27.

(28) Ali, N. Thermodynamic functions of the benzoic acid, phthalic acid and salicylic acid. *Indian J. Phys.* **1983**, *B57*, 413–419.

(29) Stull, D. R.; Westrum, E. F.; Sinke, G. C. *The Chemical Thermodynamics of Organic Compounds*; Wiley: New York, 1969.

(30) Frenkel, M.; Kabo, G. J.; Marsh, K. N.; Roganov, G. N.; Wilhoit, R. C. *Thermodynamics of organic compounds in the gas state*. Thermodynamics Research Center, Texas A&M University: College Station, Texas, 1994.

(31) Pross, A.; Radom, L.; Taft, R. W. Theoretical approach to substituent effects. Phenols and phenoxide ions. *J. Org. Chem.* **1980**, *45*, 818–826.

(32) George, P.; Trachtman, M.; Bock, C. W.; Brett, A. M. Homodesmotic reactions for the assessment of stabilization energies in benzenoid and other conjugated cyclic hydrocarbons. *J. Chem. Soc., Perkin Trans. 2* **1976**, 1222–1227.

(33) Hehre, W. J.; Ditchfield, R.; Radom, L.; Pople, J. A. Molecular orbital theory of the electronic structure of organic compounds. V. Molecular theory of bond separation. *J. Am. Chem. Soc.* **1970**, *92*, 4796–4801.

(34) Becke, A. D. Density-functional exchange-energy approximation with correct asymptotic behavior. *Phys. Rev. A* **1988**, *38*, 3098–3100.

(35) Lee, C.; Yang, W.; Parr, R. G. Development of the Colle-Salvetti correlation-energy formula into a functional of the electron density. *Phys. Rev. B* **1988**, *37*, 785–789.

(36) Becke, A. D. Density-functional thermochemistry. III. The role of exact exchange. *J. Chem. Phys.* **1993**, *98*, 5648–5652.

(37) Perdew, J. P. Density-functional approximation for the correlation energy of the inhomogeneous electron gas. *Phys. Rev. B* **1986**, *33*, 8822–8824.

(38) McLean, A. D.; Chandler, G. S. Contracted Gaussian basis sets for molecular calculations. I. Second row atoms, Z = 11−18. *J. Chem. Phys.* **1980**, *72*, 5639–5648.

(39) Krishnan, R.; Binkley, J. S.; Seeger, R.; Pople, J. A. Self-consistent molecular orbital methods. XX. A basis set for correlated wave functions. *J. Chem. Phys.* **1980**, *72*, 650–654.

(40) Schaefer, A.; Horn, H.; Ahlrichs, R. Fully optimized contracted Gaussian-basis sets for atoms Li to Kr. *J. Chem. Phys.* **1992**, *97*, 2571–2577.

(41) Schaefer, A.; Huber, C.; Ahlrichs, R. Fully optimized contracted Gaussian basis sets of triple zeta valence quality for atoms Li to Kr. *J. Chem. Phys.* **1994**, *100*, 5829–5835.

(42) Kendall, R. A.; Dunning, T. H., Jr.; Harrison, R. J. Electron affinities of the first-row atoms revisited. Systematic basis sets and wave functions. *J. Chem. Phys.* **1992**, *96*, 6796–6806.

(43) Møller, C.; Plesset, M. S. Note on an approximation treatment for many-electron systems. *Phys. Rev.* **1934**, *46*, 618–622.

(44) Irikura, K. K. *THERMO PL*; National Institute of Standards and Technology: Gaithersburg, MD, 2002.

(45) Frisch, M. J.; Trucks, G. W.; Schlegel, H. B.; Scuseria, G. E.; Robb, M. A.; Cheeseman, J. R.; Montgomery, J. A., Jr.; Vreven, T.; Kudin, K. N.; Burant, J. C.; Millam, J. M.; Iyengar, S. S.; Tomasi, J.; Barone, V.; Mennucci, B.; Cossi, M.; Scalmani, G.; Rega, N.; Petersson, G. A.; Nakatsuji, H.; Hada, M.; Ehara, M.; Toyota, K.; Fukuda, R.; Hasegawa, J.; Ishida, M.; Nakajima, T.; Honda, Y.; Kitao, O.; Nakai, H.; Klene, M.; Li, X.; Knox, J. E.; Hratchian, H. P.; Cross, J. B.; Adamo, C.; Jaramillo, J.; Gomperts, R.; Stratmann, R. E.; Yazyev, O.; Austin, A. J.; Cammi, R.; Pomelli, C.; Ochterski, J. W.; Ayala, P. Y.; Morokuma, K.; Voth, G. A.; Salvador, P.; Dannenberg, J. J.; Zakrzewski, V. G.; Dapprich, S.; Daniels, A. D.; Strain, M. C.; Farkas, O.; Malick, D. K.; Rabuck, A. D.; Raghavachari, K.; Foresman, J. B.; Ortiz, J. V.; Cui, Q.; Baboul, A. G.; Clifford, S.; Cioslowski, J.; Stefanov, B. B.; Liu, G.; Liashenko, A.; Piskorz, P.; Komaromi, I.; Martin, R. L.; Fox, D. J.; Keith, T.; Al-Laham, M. A.; Peng, C. Y.; Nanayakkara, A.; Challacombe, M.; Gill, P. M. W.; Johnson, B.; Chen, W.; Wong, M. W.; Gonzalez, C.; Pople, J. A. *Gaussian 03, Revision A.1*; Gaussian, Inc.: Pittsburgh PA, 2003.

(46) Adedeji, F. A.; Lalage, D.; Brown, S.; Connor, J. A.; Leung, M. L.; Paz-Andrade, I. M.; Skinner, H. A. Thermochemistry of arene chromium tricarbonyls and the strenghts of arene-chromium bonds. *J. Organomet. Chem.* **1975**, *97*, 221–228.

(47) Sinnokrot, M. O.; Sherrill, C. D. Density functional theory predictions of anharmonicity and spectroscopic constants for diatomic molecules. *J. Phys. Chem. A* **2001**, *115*, 2439–2448.

(48) Neugebauer, J.; Hess, B. A. Fundamental vibrational frequencies of small polyatomic molecules from density-functional calculations and vibrational perturbation theory. *J. Chem. Phys.* **2003**, *118*, 7215–7225.

(49) Dunning, T. H., Jr. Gaussian basis sets for use in correlated molecular calculations. I. The atoms boron through neon and hydrogen. *J. Chem. Phys.* **1989**, *90*, 1007–1023.

(50) Woon, D. E.; Dunning, T. H., Jr. Gaussian basis sets for use in correlated molecular calculations. III. The atoms aluminum through argon. *J. Chem. Phys.* **1993**, *98*, 1358–1371.

(51) Antony, J.; von Helden, G.; Meijer, G.; Schmidt, B. Anharmonic midinfrared vibrational spectra of benzoic acid monomer and dimer. *J. Chem. Phys.* **2005**, *123*, 014305-1−14305-11.

(52) Andersson, M. P.; Uvdal, P. New scaling factors for harmonic vibrational frequencies using the B3LYP density functional method with the triple-ζ basis set 6-311+G(d,p). *J. Phys. Chem. A* **2005**, *109*, 2937–2941.

(53) Halls, M. D.; Velkovski, J.; Schlegel, H. B. Harmonic frequency scaling factors for Hartree-Fock, S-VWN, B-LYP, B3-LYP, B3-PW91 and MP2 with the Sadlej pVTZ electric property basis set. *Theor. Chem. Acc.* **2001**, *105*, 431–421.

(54) Sinha, P.; Boesch, S. E.; Gu, C.; Wheeler, R. A.; Wilson, A. K. Harmonic vibrational frequencies: scaling factors for HF, B3LYP, and

MP2 methods in combination with correlation consistent basis sets. *J. Phys. Chem. A* **2004**, *108*, 9213–9217.

(55) Merrick, J. P.; Moran, D.; Radom, L. An evaluation of harmonic vibrational frequency scale factors. *J. Phys. Chem. A* **2007**, *111*, 11683–11700.

(56) Pfaendtner, J.; Yu, X.; Broadbelt, L. J. The 1-D hindered rotor approximation. *Theor. Chem. Acc.* **2007**, *118*, 881–898.

(57) East, A. L. L.; Radom, L. Ab initio statistical thermodynamical models for the computation of third-law entropies. *J. Chem. Phys.* **1997**, *106*, 6655–6674.

(58) Aubanel, E. E.; Robertson, S. H.; Wardlaw, D. M. Hindered rotor model for radical association reactions. *J. Chem. Soc., Faraday Trans.* **1991**, *87*, 2291–2297.

(59) Robertson, S. H.; Wardlaw, D. M. The unimolecular dissociation of the iso-propyl radical. *Chem. Phys. Lett.* **1992**, *199*, 391–396.

(60) Robertson, S. H.; Wagner, A. F.; Wardlaw, D. M. Canonical flexible transition state theory revisited. *J. Chem. Phys.* **1995**, *103*, 2917–2928.

(61) Robertson, S. H.; Wagner, A. F.; Wardlaw, D. M. Canonical flexible transition-state theory for generalized reaction paths. *Faraday Discuss.* **1995**, *102*, 65–83.

(62) Gang, J.; Pilling, M. J.; Robertson, S. H. Partition functions and densities of states for butane and pentane. *J. Chem. Soc., Faraday Trans.* **1996**, *92*, 3509–3518.

(63) Gang, J.; Pilling, M. J.; Robertson, S. H. Asymmetric internal rotation: Application to the 2-$C_4H_9CH_3$ + C_3H_6 reaction. *J. Chem. Soc., Faraday Trans.* **1997**, *93*, 1481–1491.

(64) Robertson, S.; Wagner, A. F.; Wardlaw, D. M. Flexible transition state theory for a variable reaction coordinate: Derivation of canonical and microcanonical forms. *J. Chem. Phys.* **2000**, *113*, 2648–2661.

(65) Robertson, S.; Wagner, A. F.; Wardlaw, D. M. Flexible transition state theory for a variable reaction coordinate: analytical expressions and an application. *J. Phys. Chem. A* **2002**, *106*, 2598–2613.

(66) Robertson, S. H.; Wardlaw, D. M.; Wagner, A. F. Flexible transition state theory for a variable reaction coordinate: Derivation of canonical and microcanonical forms with angular momentum conservation. *J. Chem. Phys.* **2002**, *117*, 593–605.

(67) Vivian, J. T.; Lehn, S. A.; Frederick, J. H. Nonlinear dynamics of torsion-rotation interactions: A model study of toluene. *J. Chem. Phys.* **1997**, *107*, 6646–6658.

(68) Van Speybroeck, V.; Van Neck, D.; Waroquier, M.; Wauters, S.; Saeys, M.; Marin, G. B. Ab Initio study of radical addition reactions: addition of a primary ethylbenzene radical to ethene (I). *J. Phys. Chem. A* **2000**, *104*, 10939–10950.

(69) Vansteenkiste, P.; Van Speybroeck, V.; Marin, G. B.; Waroquier, M. Ab Initio calculation of entropy and heat capacity of gas-phase n-alkanes using internal rotations. *J. Phys. Chem. A* **2003**, *107*, 3139–3145.

(70) Tafipolsky, M.; Schmid, R. Calculation of rotational partition functions by an efficient Monte Carlo importance sampling technique. *J. Comput. Chem.* **2005**, *26*, 1579–1591.

(71) Chao, J.; Zwolinski, B. J. Ideal gas thermodynamic properties of methanoic and ethanoic acids. *J. Phys. Chem. Ref. Data* **1978**, *7*, 363–377.

(72) Chao, J.; Hall, K. R.; Marsh, K. N.; Wilhoit, R. C. Thermodynamic properties of key organic oxygen compounds in the carbon range C_1 to C_4. Part 2. Ideal Gas Properties. *J. Phys. Chem. Ref. Data* **1986**, *15*, 1369–1436.

(73) Ayala, P. Y.; Schlegel, H. B. Identification and treatment of internal rotation in normal mode vibrational analysis. *J. Chem. Phys.* **1998**, *108*, 2314–2325.

(74) Senent, M. L. Ab initio determination of the torsional spectra of acetic acid. *Mol. Phys.* **2001**, *99*, 1311–1321.

(75) Kemp, J. D.; Pitzer, K. S. The entropy of ethane and the third law of thermodynamics hindered rotation of methyl groups. *J. Am. Chem. Soc.* **1937**, *59*, 276–279.

(76) Chao, J.; Wilhoit, R. C.; Zwolinski, B. J. Ideal gas thermodynamic properties of ethane and propane. *J. Phys. Chem. Ref. Data* **1973**, *2*, 427–437.

(77) Anastasakos, L.; Wildman, T. A. The effect of internal rotation on the methyl CH-stretching overtone spectra of toluene and the xylenes. *J. Chem. Phys.* **1993**, *99*, 9453–9459.

(78) Scott, D. W.; Guthrie, G. B.; Messerly, J. F.; Todd, S. S.; Berg, W. T.; Hossenlopp, I. A.; McCullough, J. P. Toluene: thermodynamic properties, molecular vibrations and internal rotations. *J. Phys. Chem.* **1962**, *66*, 911–914.

(79) Draeger, J. A. The methylbenzenes II. Fundamental vibrational shifts, statistical thermodynamic functions, and properties of formation. *J. Chem. Thermodyn.* **1985**, *17*, 263–275.

(80) Janz, G. J. *Thermodynamic Properties of Organic Compounds. Estimation Methods, Principles and Practice*; Academic Press: New York, 1967.

(81) Irikura, K. K. *Computational Thermochemistry: Prediction and Estimation of Molecular Thermodynamics*; Irikura, K. K., Frurip, D. J., Eds.; ACS Symposium Series 677; American Chemical Society: Washington, DC, 1998.

(82) Chao, J.; Hall, K. R.; Yao, J.-M. Chemical thermodynamic properties of toluene, o-, m- and p-xylenes. *Thermochim. Acta* **1984**, *72*, 323–334.

(83) Nelson, M. R.; Borkman, R. F. Internal rotation barriers: ab initio calculations on substituted ethyl benzoates and benzoic acids as models for polyester flexibility. *J. Mol. Struct.* **1998**, *432*, 247–255.

(84) Gurvich, L. V.; Veyts, I. V.; Alcock, C. B. *Thermodynamic Properties of Individual Substances*, 4th ed.; Hemisphere: New York, 1989; Vols. 1 and 2.

(85) Thermodynamics Research Center. *Selected Values of Properties of Chemical Compound*; Thermodynamics Research Center, Texas A&M University: College Station, Texas, 1997.

(86) Joback, K. G.; Reid, R. C. Estimation of Pure-Component Properties from Group-Contributions. *Chem. Eng. Commun.* **1987**, *57*, 233–243.

(87) McQuarrie, D. A.; Simon, J. D. *Physical chemistry: a molecular approach*; University Science Books: Sausalito, CA, 1997; Chap. 18, p 21.

(88) Kaji, K.; Tochigi, K.; Misawa, Y.; Suzuki, T. An adiabatic calorimeter for samples of mass less than 0.1 g and heat capacity measurements on benzoic acid at temperatures from 19 to 312 K. *J. Chem. Thermodyn.* **1993**, *25*, 699–709.

(89) Ribeiro da Silva, M. A. V.; Monte, M. J. S.; Santos, L. M. N. B. F. The design, construction, and testing of a new Knudsen effusion apparatus. *J. Chem. Thermodyn.* **2006**, *38*, 778–787.

(90) Precomputed vibrational scaling factors. Computational Chemistry Comparison and Benchmark Database (CCCBDB), released by National Institute of Standards and Technology (http://www.nist.gov). http://srdata.nist.gov/cccbdb/vibscalejust.asp (accessed Nov 24, 2009).